

Ion outflow observed by IMAGE: Implications for source regions and heating mechanisms

S. A. Fuselier¹, A. G. Ghielmetti¹, T. E. Moore², M. R. Collier², J. M. Quinn³, G. R. Wilson⁴, P. Wurz⁵, S. B. Mende⁶, H. U. Frey⁶, C. Jamar⁷, J.-C. Gerard⁸, J. L. Burch⁹

¹ Lockheed Martin Advanced Technology Center, Palo Alto, CA

² Goddard Space Flight Center, Greenbelt, MD

³ University of New Hampshire, Durham, NH

⁴ Mission Research Corporation, Nashua, NH

⁵ University of Bern, Bern, Switzerland

⁶ University of California, Berkeley, CA

⁷ Centre Spatiale de Liège, Liège, Belgium

⁸ University of Liège, Liège, Belgium

⁹ Southwest Research Institute, San Antonio, TX

Abstract: Images of the Earth's proton aurora from the IMAGE spacecraft on 8 June 2000

indicate a temporally and spatially isolated ionospheric response to a shock that impinged on the Earth's magnetopause. Sometime after this ionospheric response, the Low Energy Neutral Atom imager on IMAGE detected enhanced ionospheric outflow. The time delay between the ionospheric response and the enhanced outflow is consistent with the travel time of ~30 eV neutral Oxygen (created by charge exchange of outflowing O⁺ with the exosphere) from the low altitude ionosphere to the spacecraft. Low altitude Joule heating would result in a time delay that exceeds 20 minutes between the ionospheric response at 120 km altitude and the enhanced ion outflow at 350 km altitude. Therefore, the prompt ionospheric outflow suggests that low altitude Joule heating is not important for initial acceleration of ionospheric O⁺ in the ionosphere.

Introduction

Since the identification of significant amounts of energetic O⁺ in the magnetosphere [Shelley et al., 1972], there has been much research on the acceleration mechanisms that permit this nominally gravitationally bound ion to exit the ionosphere. To date, statistical analysis of in situ observations have demonstrated that ion outflow is solar cycle [Yau et al., 1985], seasonal [Collin et al., 1998], and magnetospheric activity dependent [Yau et al., 1985]. These and other studies of individual outflow events have indicated that acceleration occurs in stages and several acceleration mechanisms are probably responsible for ion outflow [e.g., André and Yau, 1997].

These studies have also characterized the ion outflow distributions. Escaping ionospheric O⁺ distributions observed at $\sim 1 R_E$ altitude have a perpendicular (to the magnetic field) temperature of ~ 10 eV and an outflow velocity of a few km/s. Fluxes at 50 (100) eV are more than 2 (5) orders of magnitude less than those at 10 eV [Moore et al., 1986]. An initial acceleration is required to create these O⁺ distributions out of the gravitationally bound ionospheric O⁺ (with a temperature of approximately 0.1 eV). Several mechanisms can produce this initial acceleration. One mechanism that has been modeled extensively is frictional (joule) heating initiated by energy input at low altitudes (e.g., ~ 120 km). Heating via collisions results in enhanced perpendicular and parallel ion temperatures. Although the models are very sensitive to the time history of the energy input [e.g., Heelis et al., 1993] and it is difficult to treat the

region below 200 km, where collisions become very important [e.g., *Gombosi and Kileen, 1987*], some significant features of this collisional heating are derived. First, delay times of ~10 min will occur between an energy input at 200 km and response of the O⁺ at the exobase at 350 km. Second, the delay time between energy input at 120 km and a response at 200 km can be significantly longer than 10 min, resulting in a total delay of >20 min between energy input at 120 km and response at 350 km. Third, impulsive heating can cause a significant increase in the ionospheric O⁺ outflow (after this >20 min delay) but causes little change in the ionospheric H⁺ outflow.

Other mechanisms can produce the initial acceleration of O⁺. One is direct heating of the topside ionosphere at ~300-350 km [e.g., *Wilson, 1994*]. This heating is similar to joule heating at lower altitudes. However, an important difference is that there is essentially no time delay between the energy input and the initiation of ion outflow since the heating occurs directly at the O⁺ exobase.

As the O⁺ distribution moves to higher altitudes in the diverging magnetic field, additional acceleration to energies >10 eV both parallel and perpendicular to the magnetic field can occur and the distribution folds along the magnetic field direction, forming conics and eventually field-aligned beams at very high altitudes [see, e.g., *Klumpar, 1986; André and Yau, 1999*]. For the purposes here, this further acceleration is not a critical issue since additional acceleration mechanisms are continuous and simply speed up the ionospheric outflow.

Distinction between initial heating mechanisms that produce a delayed acceleration and those that produce a prompt acceleration require ion outflow measurements on timescales of a few minutes. This distinction is difficult using in situ measurements because the spacecraft moves across magnetic field lines where outflow can occur during a potential delay time of 10-20 min. This always produces the ambiguity that outflow may occur on field lines other than the ones that the in situ spacecraft is sampling. Thus, although it has been argued from in situ measurements that the ionospheric outflow is prompt [e.g., Moore et al., 1999], this suggestion has not been conclusively verified.

The launch of the IMAGE mission, with its auroral imaging capabilities and new capability to image ionospheric ion outflow provides a unique opportunity to test initial ionospheric acceleration mechanisms. The purpose of this paper is to use these new imaging capabilities to investigate the timing between an impulsive input of energy into the ionosphere and the resulting ionospheric outflow.

Observations

IMAGE was launched on 25 March 2000 into a polar $7.2 R_E \times 1000$ km altitude elliptical orbit with initial apogee at ~ 12 LT and $\sim 40^\circ$ GSE latitude. The spacecraft carries a variety of neutral atom, radio plasma, and photon imagers [Burch et al., 1999] including a Far Ultraviolet

(FUV) Imager that makes the first global images of Doppler-shifted Lyman alpha emissions produced by energetic proton precipitation [*Mende et al.*, 1999]. Among the neutral atom imagers is a low energy neutral atom (LENA) imager which images ionospheric outflow in the energy range of 10 - 300 eV [*Moore et al.*, 1999].

The passage of a CME produced shock on 8 June 2000 provided an excellent opportunity to investigate outflow resulting from impulsive energy input into the ionosphere. At 0945 UT, the IMAGE spacecraft was at an altitude of $\sim 6.6 R_E$ on the dawn flank of the magnetosphere. The location rotated into the $(Y^2+Z^2)^{1/2} - X_{GSM}$ plane along with the TY96 magnetic field is shown in Figure 1.

At 0905 UT, the CME produced shock passed the Wind spacecraft, located at $+40 R_E$ X_{GSM} from the Earth. The solar wind velocity increased from 550 km/s to 700 km/s and the ion density increased from 2.5 cm^{-3} to 15 cm^{-3} across the shock front, resulting in an abrupt and substantial increase in the solar wind dynamic pressure. Given the X_{GSM} location of the Wind spacecraft and the solar wind speed, the disturbance propagating to and through the bow shock, across the magnetosheath to the magnetopause, and down the magnetic field line in the cusp would arrive at the ionosphere $\sim 6-9$ min after the shock front passed the Wind spacecraft.

Figure 2 shows two consecutive FUV images of the proton aurora ($>1218\text{\AA}$ Doppler-shifted Lyman-alpha emissions). The first image, at 0910:30 UT, shows weak auroral emissions with a slight enhancement near 12 LT. The second image (at 0912:30 UT) shows significant

brightening at different latitudes but confined to the dayside region near 12 LT. This dramatic increase in the proton aurora coincides with the estimated arrival of the disturbance in the ionosphere that was produced by the interplanetary shock interaction with the magnetopause. The increase in emissions, likely produced by the precipitation of both magnetospheric and solar wind protons, provides a large, spatially distinct, and impulsive energy input into the ionosphere. Subsequent images (not shown) indicate decreased emissions near 12 LT and an overall brightening of the auroral oval.

Figure 3 shows the time history of the countrate from the Earth direction in the Oxygen time of flight channels of the LENA instrument. Prior to 0912 UT, the countrate in the Oxygen channels was consistent with background. A sharp increase in the countrate is seen at 0912:36 UT, coincident with the increase in the auroral emissions in Figure 2. A much larger increase in the countrate occurs 37.5 min after the brightening of the proton aurora.

Figure 4 shows two consecutive images of neutral Oxygen from the LENA imager from 0948 and 0950 UT, that is starting one spin (2 min) before the sharp increase in the Oxygen countrate in Figure 3. The dramatic increase in the Oxygen countrate in Figure 3 at 0950 UT comes from a region near, but slightly off the Earth direction.

The LENA imager uses conversion of low energy neutrals into negative ions at a conversion surface and subsequent electrostatic analysis of the negative ion [Wurz *et al.*, 1993]. With this detection technique, the instrument is susceptible to a variety of backgrounds [e.g.,

Ghielmetti et al., 1994]. For example, there is an initial increase in the Oxygen countrate in Figure 3 coincident with the increase in the auroral emissions at 0912:30 UT in Figure 2. This countrate could be caused by an increase in the ultraviolet light from the bright aurora in Figure 2. Ultraviolet light can create negative ions through the release of photo-electrons and subsequent electron attachment to a neutral in the residual gas inside the instrument. If this electron attachment occurs near the conversion surface and the negative ions have an energy of a few eV, then they will contribute to the instrument background. This background will be strongly correlated with photon flux. In addition, high energy (several keV) neutral H can sputter heavy negative ions with energies of a few eV off the conversion surface. These sputtered ions will be strongly correlated with the background energetic H flux. Thus, the initial signal at 0912:36 UT in Figure 3 may not be Oxygen outflow from the ionosphere due to the impulsive energy input into the ionosphere seen in Figure 2.

In contrast, the dramatic increase in the Oxygen countrate at 0950 UT in Figure 3 has no corresponding increase in auroral photon intensity for the entire period between 0912:30 and 0950 UT (not shown). This increase also does not have an associated rapid increase in the neutral Hydrogen countrate of comparable magnitude (also not shown).

The LENA instrument was designed with relatively crude energy resolution within the energy passband. Unfortunately, problems with the energy discrimination in the LENA instrument result in the inability to measure the Oxygen energy for this time period. Fortunately,

the ion optics and the voltage settings of the instrument limit the incident neutral energy to a relatively narrow window between 10 eV and ~150 eV in the normal detection process (i.e., conversion of the incident low energy neutral Oxygen into negative ions and subsequent analysis of these ions within the instrument). However, as discussed above, energetic neutrals could sputter negative ions from the conversion surface. This and other possible backgrounds will be considered in the discussion section.

Here, it is assumed that the sharp increase in the Oxygen count rate at 0950 UT was caused by an increase in the neutral Oxygen flux between 10 and 150 eV. Neutrals with these energies are created by charge exchange of the ionospheric O^+ outflow with the Earth's exosphere. With this assumption, the travel times from the ionosphere to the spacecraft (a distance of $6.6 R_E$, see Figure 1) for different energy neutrals is shown in Table 1.

Within the nominal passband of the instrument, Oxygen travel times vary from 15 min to 1 hour. Since the H energy passband of the instrument is the same, H travel times are simply a factor of 4 smaller in Table 1. The 37.5 min delay between the ionospheric disturbance and the large increase in the Oxygen signal in Figure 3 is consistent with the travel time of 30 eV Oxygen neutrals from the ionosphere to the spacecraft. For this energy neutral, there is no delay between the ionospheric disturbance and the initiation of ionospheric outflow.

Discussion

Figure 2 shows that there was a localized response in the ionosphere due to the compression of the magnetosphere by a CME shock front. The ionosphere is disturbed over a considerable range of latitude but a relatively small range of local time near 12 LT. Neutral atom observations from the IMAGE spacecraft, located $6.6 R_E$ from this ionospheric disturbance, show a dramatic increase in the Oxygen channel count rate from the general direction of the Earth (Figure 4). This increase occurs 37.5 min after the ionospheric disturbance, consistent with the travel time of 30 eV neutral Oxygen from the ionosphere to the spacecraft (Table 1). If the increased count rate is due to these energy neutrals, then there is no time delay between the ionospheric disturbance and the initiation of ion outflow from the ionosphere.

Because the LENA imager does not have energy resolution in its 10 -150 eV energy passband, it is possible that the 37.5 min time delay could be accounted for by a delay in the initiation of the ion outflow and the travel time of higher energy neutral Oxygen or Hydrogen (see Table 1). Energetic Hydrogen can produce measurable counts in the Oxygen channels of the instrument by sputtering of negative heavy ions off the conversion surface. As discussed above, heavy ion sputtering by Hydrogen could have caused the increase in the Oxygen channel count rate at 0912:30 UT in Figure 3, coincident with the arrival time of the ionospheric disturbance.

While there is no direct evidence from the IMAGE observations in Figures 2 through 4 to discount the possibility that higher energy neutrals cause the increased countrate at 0950 UT, results from previous ion outflow studies using modeling and in situ observations suggest that this is not the case. Modeling of the ionospheric response to an impulsive heating event indicates that there is a significant response from ionospheric O⁺ but essentially no response by ionospheric H⁺ [Gombosi and Kileen, 1987]. Furthermore, there was no corresponding increase in the H countrate at 0950 UT, coincident with the Oxygen countrate increase. Thus, it is likely that the increase in the countrate at 0950 UT is due to direct detection of ionospheric Oxygen and not H sputtering of Oxygen off the conversion surface.

Neutral Oxygen is produced by charge exchange of the outflowing O⁺ distribution with the Earth's exosphere. In situ observations indicate that the outflowing O⁺ distribution from the ionosphere has a relatively low temperature (~10 eV) and fluxes at 50 (100) eV are more than 2 (5) orders of magnitude less than that those 10 eV [Moore et al., 1986]. These observations suggest that the neutral Oxygen observed by LENA at 0950 UT had an energy less than 50 eV.

As discussed in the introduction, the thermal pulse caused by Joule heating at 120 km altitude requires considerable time (>20 min) to propagate to the O⁺ exobase at 350 km and cause heating at that location. Thus, there will be a >20 min time delay between the ionospheric disturbance and the initiation of ion outflow. In contrast, the timing of the ionospheric disturbance and the arrival of ~30 eV neutrals (charge exchanged from outflowing O⁺) at the

spacecraft does not allow for any delay between the ionospheric disturbance and the initiation of ion outflow.

Direct heating of the topside ionosphere at 350 km by the ionospheric disturbance will result in prompt ionospheric outflow [e.g., Wilson, 1994]. Therefore, the timing results in this paper suggest that topside ionospheric heating is the dominant mechanism producing the increased ionospheric outflow observed by LENA. This does not rule out Joule heating at lower altitudes as a possible source of sustained ionospheric outflow. However, direct topside ionospheric heating or some similar mechanism appears to be providing the magnetosphere with significant and nearly instantaneous ionospheric outflow in response to the passage of a CME shock.

Acknowledgments: The authors thank W. K. Peterson for his helpful comments. Solar wind data was obtained from the CDAWeb from Dr. K. Ogilvie. Research on the IMAGE mission is supported by NASA contract to Southwest Research Institute and subcontracts to participating IMAGE institutions.

References

André, M., and Yau, A. L., Theories and observations of ion energization and outflow in the high latitude magnetosphere, *Space Sci. Rev.*, 80, 27, 1997.

Burch, J. L., IMAGE mission overview, *Space Sci. Rev.*, 91, 1, 2000.

Collin, H. L., W. K. Peterson, O. W. Lennartsson, J. F. Drake, The seasonal variation of auroral ion beams, *Geophys. Res. Lett.*, 25, 4071, 1998.

Ghielmetti, A. G., E. G. Shelley, S. A. Fuselier, P. Wurz, P. Bochsler, F. A. Herrero, M. F. Smith, and T. S. Stephen, Mass spectrograph for imaging low-energy neutral atoms, *Optical Eng.*, 33, 362, 1994.

Gombosi, T. I., and T. L. Kileen, Effects of thermospheric motions of the polar wind: A time-dependent numerical study, *J. Geophys. Res.*, 92, 4725, 1987.

Heelis, R. A., G. J. Bailey, R. Sellek, R. J. Moffett, and B. Jenkins, Field-aligned drifts in subauroral ion drift events, *J. Geophys. Res.*, 98, 21493, 1993.

Klumpar, D. M., A digest and comprehensive bibliography on transverse auroral ion acceleration, in *Ion Acceleration in the Magnetosphere and Ionosphere*, Geophys. Monogr., American Geophysical Union, 389, 1986.

Mende, S. B., et al., Far ultraviolet imaging from the IMAGE spacecraft: 3. Spectral imaging of Lyman-alpha and OI 135.6 nm, *Space Sci. Rev.*, 287, 2000.

Moore, T. E., M. Lockwood, M. O. Chandler, J. H. Waite Jr., C. R. Chappell, A. Persoon, and M. Sugiura, Upwelling O⁺ ion source characteristics, *J. Geophys. Res.*, 91, 7019, 1986.

Moore, T. E., et al., The low energy neutral atom imager for IMAGE, *Space Sci. Rev.*, 155, 2000.

Shelley, E. G., Johnson, R. D., and R. D. Sharp, Satellite observations of energetic heavy ions during a geomagnetic storm, *J. Geophys. Res.*, 77, 6104, 1972.

Wilson, G. R., Kinetic modeling of O⁺ upflows resulting from ExB convection heating in the high-latitude F region ionosphere, *J. Geophys. Res.*, 99, 17453, 1994.

Wurz, P., et al., Concept of the HI-LITE Neutral Atom Imaging Instrument, Proceedings of the Symposium on Surface Science, eds. P. Varga, and G. Betz, pp. 225-230, Kaprun, Austria, 1993.

Yau, A. W., Shelley, E. G., Peterson, W. K., and L. Lenchyshyn, Energetic auroral and polar ion outflow at DE-1 altitudes: Magnitude, composition, magnetic activity dependence and long-term variations, *J. Geophys. Res.*, 90, 8417, 1985.

Table 1: Travel Times for Neutrals from the Ionosphere

Energy (eV)	O Travel Time (min)	H Travel Time (min)
10	64.4	16.2
30	37.1	9.3
50	28.5	7.2
100	20.3	5.1
150	16.6	4.1

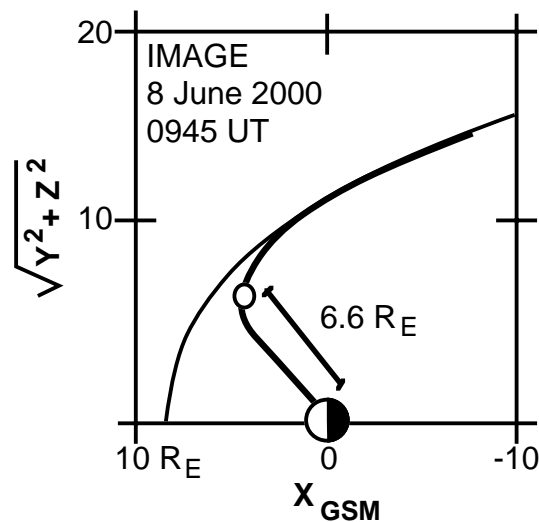


Figure 1. The location of the IMAGE spacecraft in the magnetosphere at the time of a passage of a CME-related shock. The spacecraft was located at approximately 9 LT, 6.25 RE from the Earth. The projection of the magnetic field line from the TY96 model is shown.

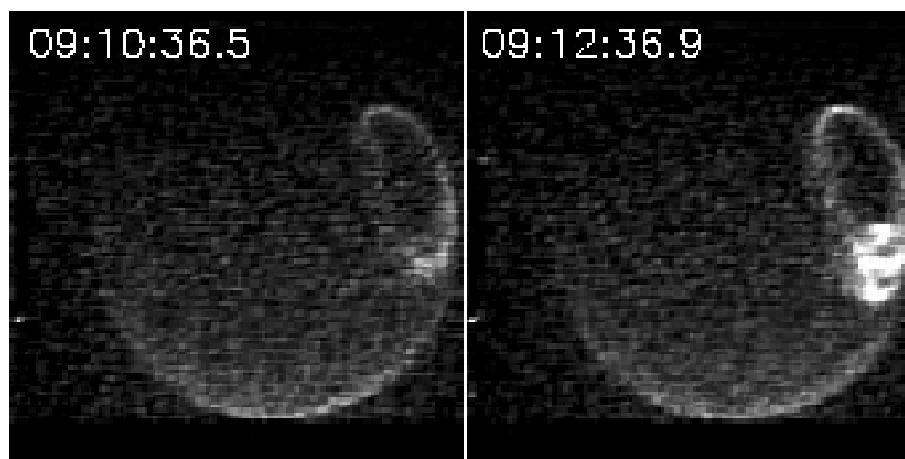


Figure 2. Two consecutive snapshots of the proton aurora (Doppler shifted Lyman-alpha emissions). The ionospheric response to the CME shock passage is evident in the second image. There is a significant and localized brightening of the emissions near 12 LT.

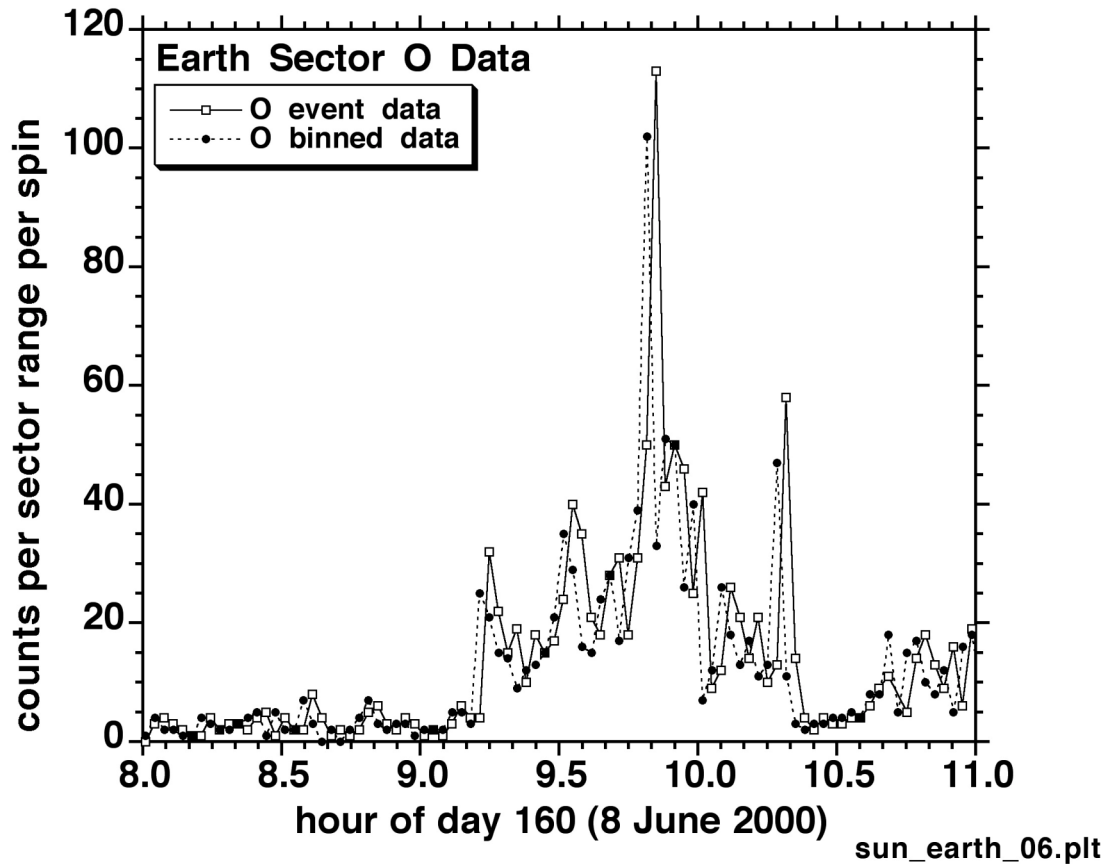


Figure 3. Time history of the countrate in the Oxygen channels of the LENA imager from the direction of the Earth. There is a prompt countrate increase at the time of the enhanced proton aurora in Figure 2. A much larger increase in the countrate is seen 37.5 min after the initial ionospheric disturbance.

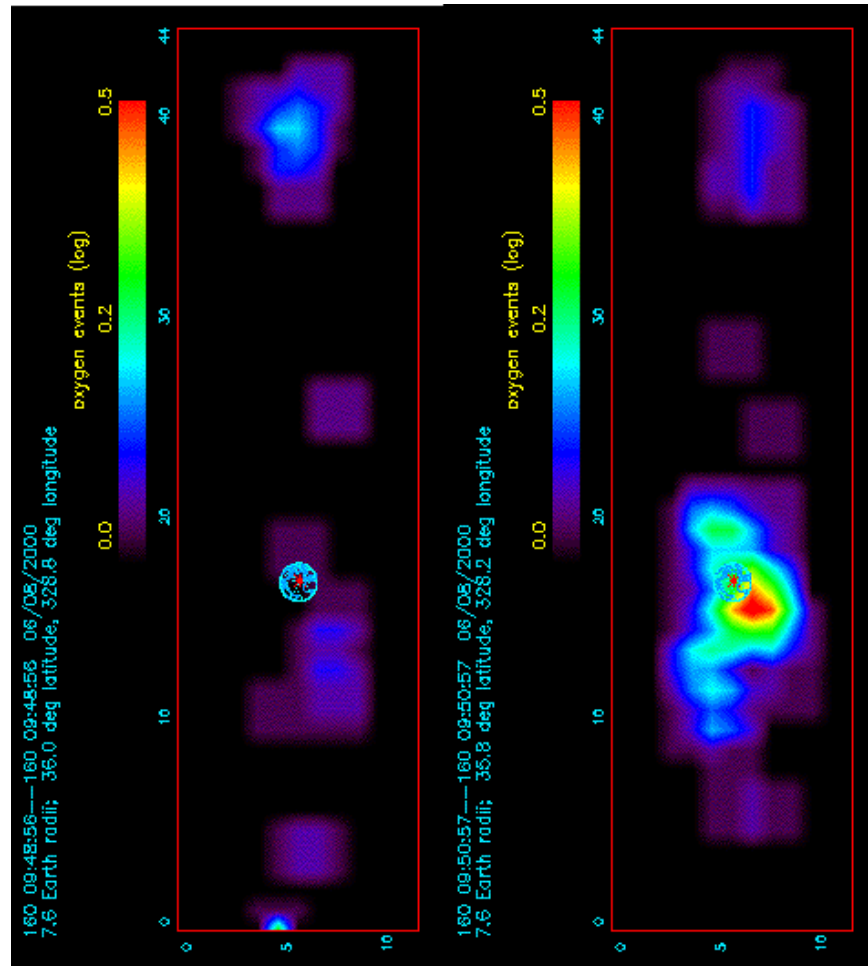


Figure 4. Two consecutive images from the LENA imager from the Earth direction.

These images show how the dramatic increase in the Oxygen countrate (Figure 3) comes from slightly off the direction of the Earth.